JOURNAL OF ASIAN CERAMIC SOCIETIES
https://doi.org/10.1080/21870764.2025.2572156

RESEARCH ARTICLE

OPEN ACCESS Check for updates

Synthesis and thermal behavior of single-phase tridymite

Yuki Maruyama[a], Yuji Hanada[a], Koki Kinami[a], Masanori Nagao[a], Satoshi Watauchi[a], Hidehiro Takahashi[b], Masataka Ohgaki[b] and Isao Tanaka[a]

[a]Center for Crystal Science and Technology, University of Yamanashi, Kofu, Japan; [b]Hitachi High-Tech Analysis Corporation, Chuo-Ku, Japan

ABSTRACT

In this study, single-phase tridymite was successfully synthesized by optimizing the mixing and reaction conditions. When amorphous SiO_2 and K_2CO_3 mineralizer were dry mixed and calcined, the cristobalite phase was formed as the main phase in addition to the tridymite phase, and the tridymite phase fraction in the samples increased with increasing reaction temperature and time. Wet mixing with ethanol improved the synthesis of single-phase tridymite. The synthesized tridymite exhibited thermal expansion and shrinkage associated with the phase transition.

ARTICLE HISTORY
Received 1 July 2025
Accepted 4 October 2025

KEYWORDS
Silicon dioxide; tridymite; refractory; thermal behavior

1. Introduction

Silicon dioxide can appear in different crystalline phases depending on the temperature during formation; primarily, these include quartz below 870°C, tridymite between 870°C and 1470°C, and cristobalite above 1470°C under atmospheric pressure [1,2]. These phases occur naturally as minerals; however, synthesis processes have also been investigated to help obtain minerals for industrial applications. In particular, single-phase tridymite is desired for high-temperature material applications owing to its excellent heat resistance. Additionally, single-phase tridymite is essential as a standard sample for X-ray diffraction to determine the free silicic acid content in airborne soil, rock, or mineral dust in working environments. The use of amorphous silica offers several advantages for industrial applications of tridymite synthesis. It has been reported that amorphous silica allows the formation of tridymite due to its high reactivity and lack of long-range order [3]. However, when synthesized from amorphous silica, single-phase tridymite has not been obtained even within the appropriate temperature range because of the phase transition from tridymite to cristobalite, unless alkali metal carbonates such as potassium carbonate are added as mineralizer [4]. The addition of a mineralizer is necessary for the synthesis of tridymite, but previous reports have not examined the effect of mixing with raw materials and mineralizers on phase formation.

Tridymite has a complex structure and contains numerous polymorphs. At room temperature, three polymorphs have been reported: monoclinic L1–T_O (MC), orthorhombic L2–T_D ($PO_{5/10}$), and monoclinic L3–T_O (MX–1) [5–10]. In addition, well-ordered tridymite L1–To (MC) transforms into an incommensurate low-tridymite, L3–To′ (= tridymite MX–13), via quenching from 150°C to below 0°C owing to thermally induced stress and grinding at ambient temperature [11]. High-temperature modifications of tridymite have also been reported, with some examples being orthorhombic H5–To, orthorhombic H4–To (OP), incommensurate orthorhombic H3–To (OS), orthorhombic H2–To (OC), and hexagonal H1–To (HP) [12–17].

To date, the absence of measurements using a single-phase tridymite has led to varied reports on the thermal behavior associated with the phase transition of tridymite. The thermal behavior of single-phase tridymite must be investigated to evaluate its applicability as a high-temperature structural material. Tridymite exhibits characteristic phase transitions accompanied by thermal expansion and shrinkage, which can significantly affect the dimensional stability and reliability of materials under thermal stress. Therefore, this study aimed to synthesize single-phase tridymite, obtain fundamental data such as the linear thermal expansion coefficient, and evaluate the thermal stability of tridymite for potential use in high-temperature applications.

In this study, the synthesis conditions of single-phase tridymite were optimized by examining the mixing process for the raw materials and the effects of calcination temperature, calcination time, and amount of mineralizer added. Furthermore, anomalous thermal behaviors, such as thermal expansion, of the synthesized single-phase tridymite were investigated, and their correlation with phase transitions is discussed.

CONTACT Yuki Maruyama myuuki@yamanashi.ac.jp Center for Crystal Science and Technology, University of Yamanashi, 7-32 Miyamae, Kofu, Yamanashi, Japan

2. Experimental procedure

Amorphous SiO_2 (Rare Metallic Co., Ltd. 99.99%, particle size approximately 10 μm) and K_2CO_3 (Rare Metallic Co., Ltd. 99.9%) were used as starting materials. 1–20 wt% of K_2CO_3 was added to SiO_2, and the mixture was dry mixed or wet mixed with distilled water or ethanol using a mortar and pestle. The mixed samples were calcined in air at 900–1200°C for 2–24 h. The calcined samples were analyzed using powder X-ray diffraction (XRD, Rigaku, SmartLab) for phase identification and scanning electron microscopy (SEM, Hitachi High-Technologies, TM3030) for morphological observations. Elemental maps were obtained using energy dispersive X-ray spectrometry (EDS, Bruker, Quantax 70).

The thermal behaviors, such as thermal expansion and calorimetric change, of single-phase tridymites were measured. The measurement samples were prepared using the following procedure. A mixture of SiO_2 and K_2CO_3 of 4 wt% was calcined at 1100°C for 12 h. The calcined samples were rinsed three times with water to remove the unreacted K_2CO_3. The potassium concentration in the rinsed samples was determined via atomic absorption spectrometry to be 0.77 wt%. After drying, the samples were formed into cylindrical rods of approximately 6 mm in diameter and 17 mm in length using the rubber press method under a hydrostatic pressure of 300 MPa at room temperature, and they were used as samples for thermal expansion measurements. A thermomechanical analyzer (Hitachi High-Tech Analysis Corporation, model TMA7300) was used to measure thermal expansion and shrinkage. Measurements were performed via heating and cooling at a load of 200 mN in nitrogen between 25°C and 1250°C at 5°C/min for three consecutive cycles. Additionally, thermal calorimetric analysis of the powdered tridymite samples was performed using differential scanning calorimetry (DSC, Hitachi High-Tech Analysis Corporation, model NEXTA DSC600) via heating and cooling continuously between −110°C and 560°C at 10°C/min in nitrogen for two cycles.

3. Results and discussion

Figure 1 shows the XRD patterns of the products prepared via dry mixing under various reaction conditions. The XRD patterns of the products agreed with the pattern for cristobalite phase (CR) reported in the ICDD data 04–008–7829 [18] and the tridymite phase (TR) reported in the ICDD data 04–008–8127 [6]. The XRD relative intensity of tridymite increased with higher calcination temperature, longer calcination time, and higher K_2CO_3 addition, suggesting an increase in the tridymite formation rate. However, single-phase tridymite was not obtained under any of the

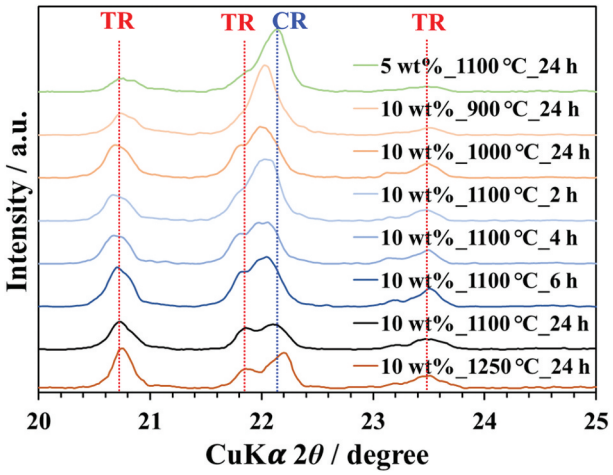

Figure 1. XRD patterns of the products prepared using dry mixing and various reaction conditions.

conditions. The calcined samples formed agglomerates, and the calcination temperature exceeded the melting point of K_2CO_3 (891°C), suggesting the occurrence of a solid – liquid reaction between molten K_2CO_3 and SiO_2. Higuchi *et al* [4]. reported that when alkali metal oxides are added to silica, a molten layer forms on part of the silica, facilitating silica crystallization and phase transitions through this layer. Thus, ensuring the uniform dispersion of K_2CO_3 mineralizer in the SiO_2 raw material during the mixing process is crucial. The mixing method was investigated in terms of this aspect.

The samples were wet-mixed using distilled water or ethanol and then calcined. Figure 2 shows the XRD patterns of the products calcined at 1100°C for 24 h under various mixing conditions with 4 wt% K_2CO_3 addition. The 4 wt% K_2CO_3 addition was considered a representative condition to evaluate the impact in this study. Single-phase tridymite was obtained in samples prepared by wet mixing, whereas it was not obtained through dry mixing. After wet mixing with distilled water, the diffraction peaks of the tridymite phase broadened, although no cristobalite phase was observed. In the calcined samples obtained from wet mixing with distilled water, the diffraction peaks of the tridymite phase broadened, although no cristobalite phase was observed. When wet mixing was conducted with distilled water, the mixed sample changed from a paste-like state to a gypsum-like lump after drying, making mixing difficult. However, wet mixing with ethanol did not harden after drying, and yielded single-phase tridymite with a small full width at half maximum (FWHM) and high X-ray diffraction intensity as shown in Figure 2(b). The FWHM value of (112) line in tridymite phase obtained with dry, distilled water, and ethanol mixing was 0.32°, 0.24°, and 0.16°, respectively. When mixed with water, likely, the K_2CO_3 particles were nonuniformly dispersed in the SiO_2 raw material owing to the agglomeration of K_2CO_3

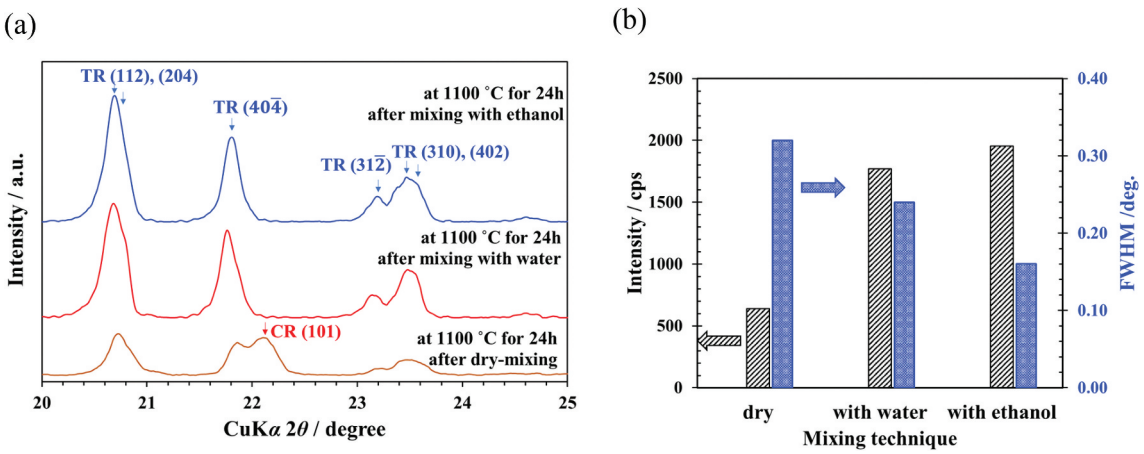

Figure 2. (a) XRD patterns of the products prepared using various mixing conditions with 4 wt% K_2CO_3 addition and (b) intensity and full width at half maximum at (112) plane.

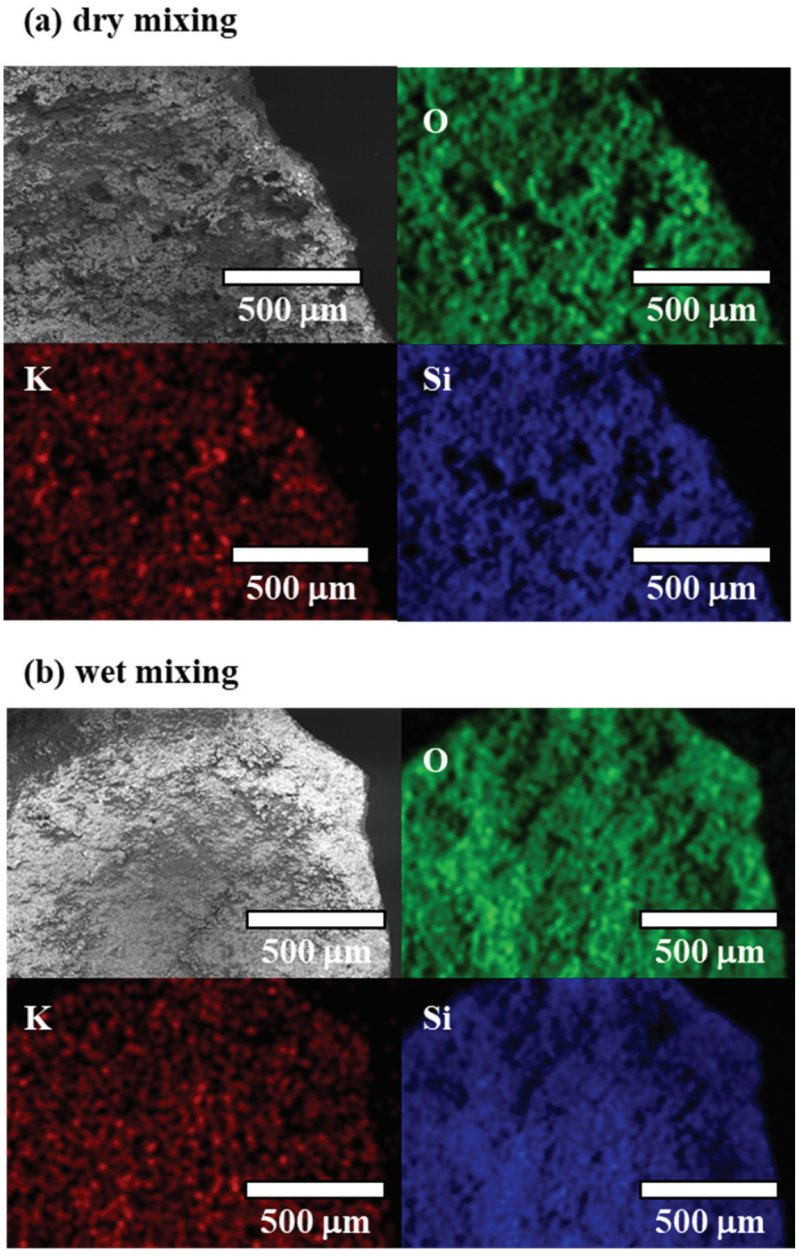

Figure 3. SEM images and EDS elemental maps of the fracture surfaces of the products prepared by (a) dry or (b) wet mixing with 4 wt% K_2CO_3 addition.

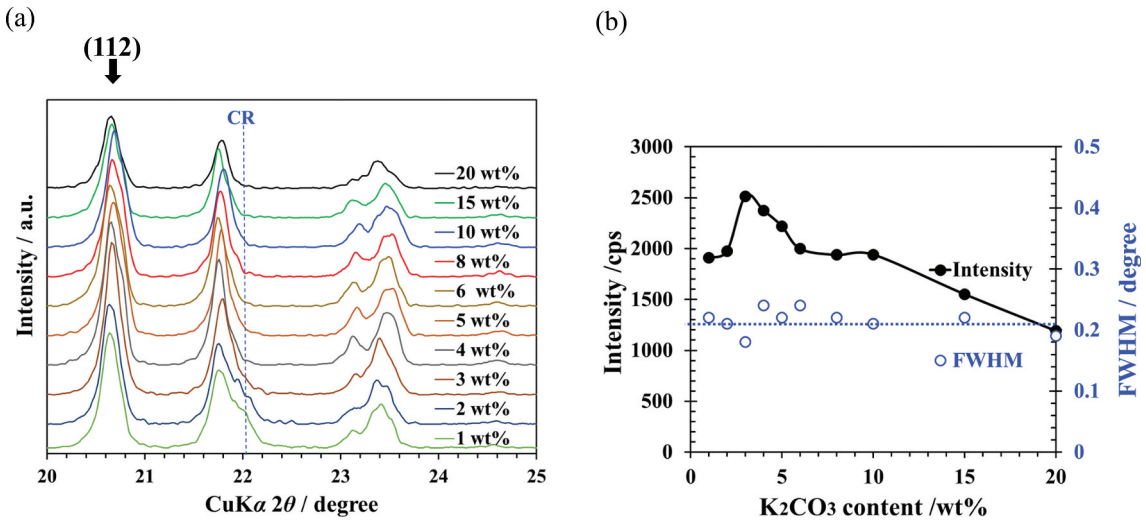

Figure 4. (a) XRD patterns of the products prepared using various amounts of K_2CO_3 addition and (b) intensity and full width at half maximum at the (112) plane.

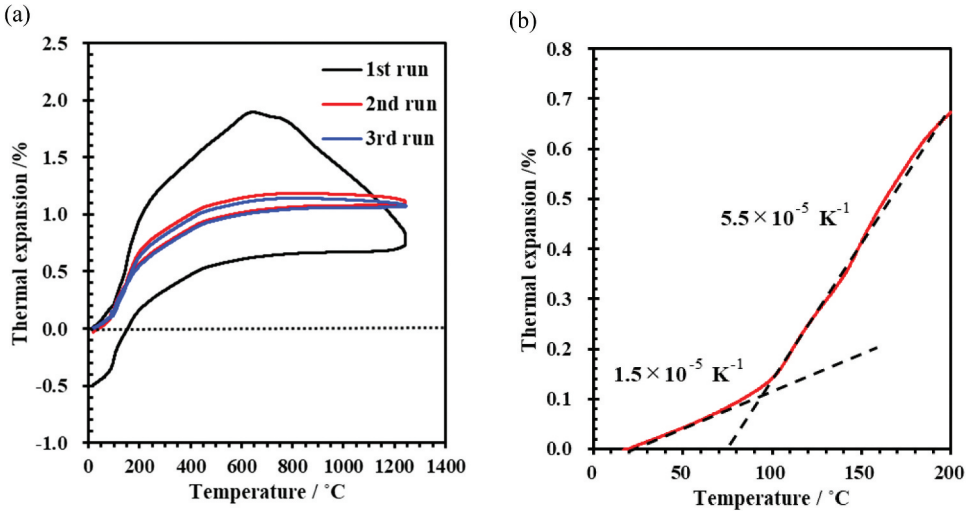

Figure 5. (a) Thermal expansion of tridymite and (b) its enlarged figure at approximately RT–200°C in the 2nd run.

particles after drying because the K_2CO_3 was dissolved in water. The SEM images and elemental maps of the fractured surfaces of the calcined samples prepared by dry mixing and by wet mixing with ethanol are shown in Figure 3. Cracks and voids of approximately 50 µm were observed in the samples prepared via dry mixing. In contrast, the samples prepared by wet mixing exhibited no cracks or voids of that size, with the particles showing greater aggregation. Compared to samples synthesized by dry mixing, K was uniformly distributed in products synthesized by wet mixing with ethanol. The enhanced particle adhesion was suggested to contribute to the improved formation of tridymite. These results suggest that ethanol mixing is optimal for the synthesis of single-phase tridymite.

Subsequently, the effects of varying amounts of K_2CO_3 additive on the products were investigated to determine the optimal quantity. The XRD patterns of the products calcined at 1100°C for 24 h after wet mixing with ethanol and different K_2CO_3 additive amounts are shown in Figure 4(a). In the products with 1 and 2 wt% K_2CO_3 addition, the cristobalite phase was obtained in addition to the tridymite phase. The tridymite single phase was obtained by adding 3 wt% or more of K_2CO_3. When 1–10 wt% K_2CO_3 was added, the peak position did not change significantly. In the products with more than 15 wt% K_2CO_3, the diffraction peaks of tridymite shifted toward lower angles. Moreover, as the K_2CO_3 additive amount increased, the diffraction intensity of tridymite decreased, indicating the possible formation of alkali silicates, although no XRD peaks of impurities were observed. Figure 4(b) shows the XRD intensity and FWHM of the (112) peaks for the products obtained with various K_2CO_3 additive amounts. The product with 3 wt% K_2CO_3 addition exhibited the highest diffraction intensity and the lowest FWHM. Thus, the optimum K_2CO_3 additive amount was determined to be 3 wt%.

Figure 5(a) depicts the thermal expansion of the unsintered tridymite molded sample, where the

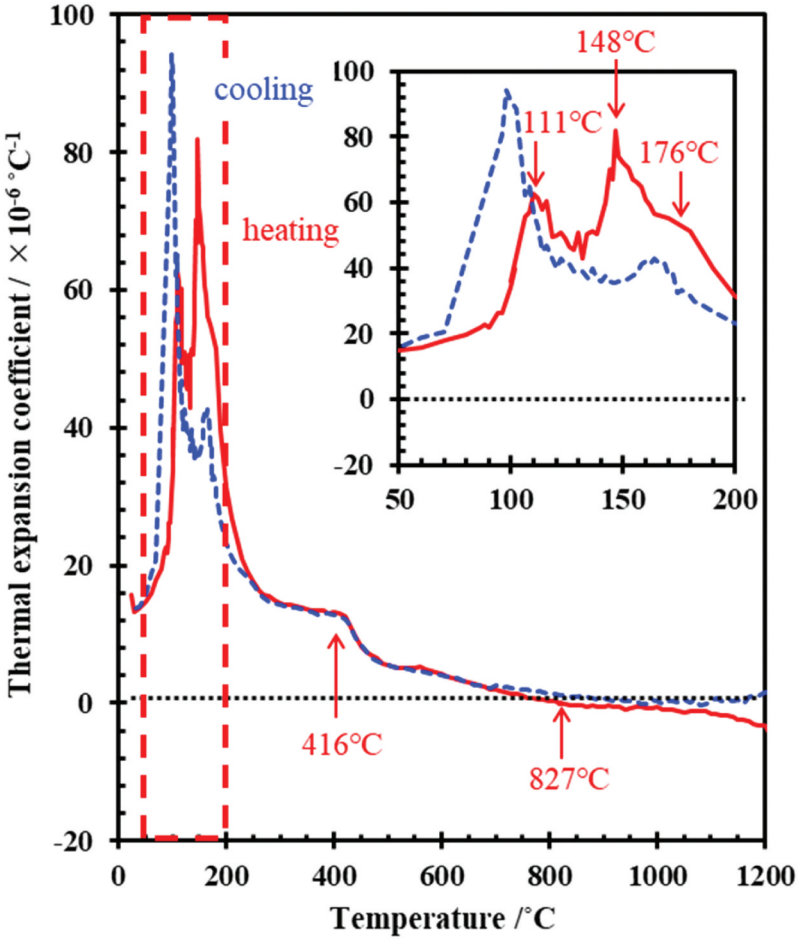

Figure 6. Thermal expansion coefficient of tridymite.

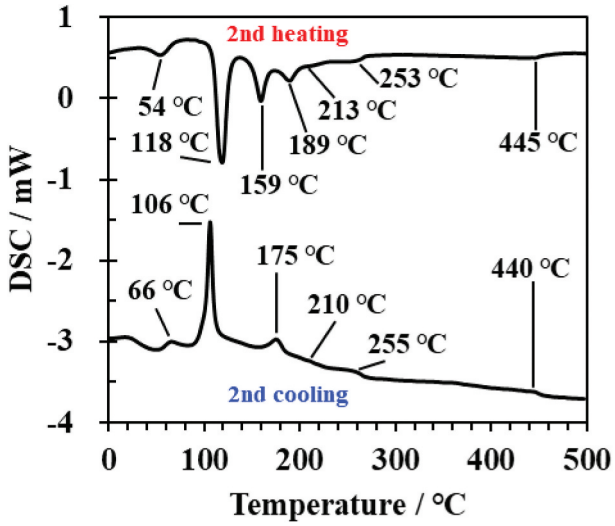

Figure 7. DSC curves of tridymite.

expansion for each heating cycle was measured relative to the sample length before each heating cycle. The molded sample exhibited sintering-induced shrinkage above 645°C at the first heating cycle. Sintering with the first heating cycle showed a shrinkage of only 0.5% at room temperature compared with before heating. The heating and cooling processes in the second and third cycles induced the same thermal behavior. Compared to the sample length at room temperature, a rapid expansion of approximately 0.5% between approximately 90°C and 200°C, a gradual expansion of approximately 1% near 500°C, an expansion of approximately 1.1% near 800°C, and a slight contraction above 800°C were observed. As shown in Figure 5(b), thermal anomalies were observed from room temperature to 200°C. During the second heating process, the average linear expansion coefficient from room temperature to 90°C was 1.5×10^{-5} K^{-1}, whereas the coefficient from 100°C to 200°C was 5.5×10^{-5} K^{-1}, more than three times higher. Additionally, the deviation from linearity in the temperature range from 100°C to 200°C was large, suggesting the presence of more complicated thermal anomalies within that temperature range.

Figure 6 presents the linear expansion coefficient during the second heating process. A sharp anomaly in the thermal expansion coefficient was observed below 200°C, confirming the change in the linear thermal expansion coefficient due to three transitions between the MC – OP, OP – OS, and OS – OC phases of tridymite at 111°C, 148°C, and 176°C, respectively [14,15,19–21]. Similar results were reported for natural tridymite [22]. Anomalous linear thermal expansion coefficients were also observed near 416°C, possibly due to the phase transition from the OC phase to the HP phase

[15,17,21]. Furthermore, the thermal shrinkage above approximately 800°C during the second heating process observed in Figure 5 was confirmed to indicate a negative linear thermal expansion coefficient above 827°C. Such phase transitions are reversible during heating and cooling processes. Further investigations, such as in-situ high-temperature X-ray diffraction, are planned in future work to clarify the changes in the crystal structure or microstructure during the thermal cycle.

Figure 7 shows the DSC curves of the tridymite powder samples. During heating, seven endothermic peaks were observed at 54°C, 119°C, 159°C, 189°C, 213°C, 253°C, and 445°C. The phase transition temperatures were slightly different from the reported phase transition temperatures because they also depended on the synthesis conditions of the sample, such as the species and amounts of impurities and the added elements, calcination temperature, and calcination time. Three phase transitions were observed in the DSC measurements in addition to the four typical phase transitions observed in the thermal expansion measurements. The peaks at 54°C, 213°C, and 253°C correspond to the MX-1–MC transition [17,21], OS – OC transition [21], and S3–S4 transition [9], respectively. The phase transition, except for near 160°C, was confirmed to be reversible owing to the exothermic peak on cooling.

4. Conclusion

Single-phase tridymite was successfully synthesized by wet mixing amorphous SiO_2 and K_2CO_3 mineralizers with ethanol and performing calcination at 1100°C for 24 h. When testing various amounts of additives, the product with 3 wt% K_2CO_3 exhibited the highest diffraction intensity and the lowest FWHM. Thermal mechanical analysis revealed a slightly negative linear thermal expansion coefficient above approximately 800°C during the second heating, with no abrupt dimensional changes up to 1200°C. DSC measurements showed reversible phase transitions upon heating and cooling, confirming good phase stability. These thermal properties of negative expansion, dimensional stability, and reversibility are advantageous for refractory applications such as thermal shock-resistant linings.

Disclosure statement

No potential conflict of interest was reported by the author(s).

Funding

This work was supported by The Technical Association of Refractories, Japan.

ORCID

Yuki Maruyama http://orcid.org/0000-0001-6094-4191
Masataka Ohgaki http://orcid.org/0000-0003-1930-9000
Isao Tanaka http://orcid.org/0000-0002-2736-7107

References

[1] Kracek FC. Polymorphism. United State: Encyclopaedia Britannica press; 1953.
[2] Sosman RB. New and old phase of silica. Trans Br Ceram Soc. 1955;54:655–670.
[3] Sano T, Shiono T. Effect of CaO addition on synthesis of tridymite phase from amorphous silica. J Soc Mater Sci Jpn. 2018;67:603–608. doi: 10.2472/jsms.67.603
[4] Higuchi M, Azuma Y. Effect of alkali metal oxide addition on crystallization and phase transformation of sintered spherical silica. J Ceram Soc Jpn. 1997;105:385–390. doi: 10.2109/jcersj.105.385
[5] Dollase WA, Baur WH. The superstructure of meteoritic low tridymite solved by computer simulation. Am Mineral. 1976;61:971–978.
[6] Kato K, Nukui A. Die kristallstruktur des monoklinen tief-tridymits. Acta Crystallogr Sec B. 1976;32(8):2486–2491.
[7] Baur WH. Silicon–oxygen bond lengths, bridging angles Si–O–Si and synthetic low tridymite. Acta Crystallogr Sec B. 1977;33(8):2615–2619. doi: 10.1107/S0567740877009029
[8] Hill VG, Roy R. Silica structure studies. V. undefined the variable inversion in cristobalite. J Am Ceram Soc. 1958;41(12):532–537. doi: 10.1111/j.1151-2916.1958.tb12911.x
[9] Sato M. Mineral xray study of tridymite (3). Unit cell dimensions and phase transition of tridymite, type S. J. 1964;4(3):215–225. doi: 10.2465/minerj1953.4.215
[10] Flörke OW, Langer K. Hydrothermal recrystallization and transformation of tridymite. Contr Mineral Petrol. 1972;36(3):221–230. doi: 10.1007/BF00371433
[11] Hoffmann W, Kockmeyer M, Löns J, et al. The transformation of monoclinic low–tridymite MC to a phase with an incommensurate superstructure. Fortshritte der Mineralogie. 1983;61:96–98. doi: 10.1002/zaac.19836180118
[12] Dollase WA. The crystal structure at 220 °C of orthorhombic high tridymite from the Steinbach meteorite. Acta Crystallogr. 1967;23(4):617–623. doi: 10.1107/S0365110X67003287
[13] Kihara K. An orthorhombic superstructure of tridymite existing between about 105 and 180 °c. Z für Kristallogr - Crystalline Mater. 1977;146(4–6):185–204. doi: 10.1524/zkri.1977.146.4-6.185
[14] Kihara K. Thermal change in unit-cell dimensions, and a hexagonal structure of tridymite. Z für Kristallogr - Crystalline Mater. 1978;148(3–4):237–254. doi: 10.1524/zkri.1978.148.1-2.237
[15] Nukui A, Nakazawa H. Thermal changes in monoclinic tridymite. Am Mineral. 1978;63:1252–1259.
[16] Nukui A, Yamomoto A, Nakazawa H. Non-integral phase in tridymite. AIP Conf Proc. 1979;53:327–329. doi: 10.1063/1.31883
[17] Graetsch H, Flörke OW. X-ray powder diffraction patterns and phase relationship of tridymite modifications. Z für Kristallogr. 1991;195(1–2):31–48. doi: 10.1524/zkri.1991.195.1-2.31

[18] Downs RT, Palmer DC. The pressure behavior of a cristobalite. Am Mineral. 1994;76:9–14.
[19] Nukui A, Nakazawa H. Polymorphism in tridymite. J Mineral Soc Jpn. 1980;14(Special2):364–386. doi: 10.2465/gkk1952.14.Special2_364
[20] Hirose T, Kihara K, Okuno M, et al. X-ray, DTA and Raman studies of monoclinic tridymite and its higher temperature orthorhombic modification with varying temperature. J Mineral Petrol Sci. 2005;100(2):55–69. doi: 10.2465/jmps.100.55
[21] Kanzaki M. Phase transitions of tridymite MC: a low frequency Raman spectroscopic study. J Mineral Petrol Sci. 2020;115(3):296–301. doi: 10.2465/jmps.191122b
[22] Austin JB. The coefficient of linear thermal expansion of tridymite. J Am Chem Soc. 1954;76(23):6019–6020. doi: 10.1021/ja01652a038